

Spectral Statistics of the Triaxial Rigid Rotator: Semiclassical Origin of their Pathological Behavior

V.R. Manfredi¹, V. Penna² and L. Salasnich^{1,3}

¹Dipartimento di Fisica "G. Galilei", Università di Padova,
Istituto Nazionale di Fisica Nucleare, Sezione di Padova,
Via Marzolo 8, 35131 Padova, Italy

²Dipartimento di Fisica, Politecnico di Torino,
Istituto Nazionale per la Fisica della Materia, Unità di Torino,
Corso Duca degli Abruzzi 24, 10129 Torino, Italy

³Dipartimento di Fisica, Università di Milano,
Istituto Nazionale per la Fisica della Materia, Unità di Milano,
Via Celoria 16, 20133 Milano, Italy

Abstract

In this paper we investigate the local and global spectral properties of the triaxial rigid rotator. We demonstrate that, for a fixed value of the total angular momentum, the energy spectrum can be divided into two sets of energy levels, whose classical analog are librational and rotational motions. By using diagonalization, semiclassical and algebraic methods, we show that the energy levels follow the anomalous spectral statistics of the one-dimensional harmonic oscillator.

1 Introduction

Berry and Tabor^{1,2} have shown that for a generic quantum system, which is classically integrable, the spectral statistics of energy levels follow the Poisson ensemble, while for a system whose classical analog is chaotic the spectral statistics follow the Gaussian Orthogonal Ensemble (GOE) of Random Matrix Theory (RMT) (for a review see Ref. 3). Nevertheless, there are some exceptions to this classical-quantum correspondence: the best known case is the harmonic oscillator one.^{4,5} Recently we have discussed another pathological case: the classically integrable triaxial rigid rotator.⁶ We have numerically computed the energy levels and then calculated the nearest-neighbor

spacing distribution $P(s)$ and the spectral rigidity $\Delta_3(L)$. We have found that $P(s)$ shows a sharp peak at $s = 1$ while $\Delta_3(L)$ for small values of L follows the Poissonian predictions and asymptotically it shows large fluctuations around its mean value.⁶ Such behavior of spectral statistics is quite similar to that of a one-dimensional harmonic oscillator. In this paper we have calculated the exact energy levels, the semiclassical ones and those obtained by an algebraic harmonic approximation. We show that, for a fixed value of the total angular momentum, the Hamiltonian of the triaxial top describes a sort of nonlinear pendulum and its semiclassical energy spectrum can be divided into two sets of energy levels, corresponding to librational and rotational motion respectively. These energy levels are close to the exact ones apart near the separatrix. Around the minima and the maxima of the classical energy, the exact energy levels are described accurately by approximate algebraic formulas.

2 Triaxial Rigid Rotator

The classical Hamiltonian H of the triaxial rigid rotator is given by

$$H = \frac{1}{2} (aJ_1^2 + bJ_2^2 + cJ_3^2) , \quad (1)$$

where $\mathbf{J} = (J_1, J_2, J_3)$ is the angular momentum of the rotation and $a = 1/I_1$, $b = 1/I_2$, $c = 1/I_3$ are three parameters such that I_1 , I_2 and I_3 are the principal momenta of inertia of the top.^{7,8} Here we choose $a < b < c$. The quantum Hamiltonian \hat{H} is obtained by replacing components J_m of the angular momentum, in the classical expression (1), by the corresponding quantum operators \hat{J}_1 , \hat{J}_2 and \hat{J}_3 . These obey the commutators $[\hat{J}_\ell, \hat{J}_k] = i \varepsilon_{\ell,j,m} \hat{J}_m$ and commute with the Casimir operator $\hat{J}^2 = \hat{J}_1^2 + \hat{J}_2^2 + \hat{J}_3^2$, namely $[\hat{J}^2, \hat{J}_k] = 0$. In view of the latter equation, a standard choice to deal with the angular-momentum dynamics consists in diagonalizing the two operators \hat{J}^2 and \hat{J}_3 within the basis $\{|j, k\rangle : |k| \leq j\}$ such that $\hat{J}_3|j, k\rangle = k\hbar|j, k\rangle$ and $\hat{J}^2|j, k\rangle = j(j+1)\hbar^2|j, k\rangle$, where the index j labels the angular-momentum representation. After recalling that $\hat{J}_\pm|j, k\rangle = [(j \mp k)(j \pm k + 1)]^{1/2}\hbar|j, k \pm 1\rangle$ (with $\hat{J}_\pm = \hat{J}_1 \pm i\hat{J}_2$), the non-zero matrix elements of the quantum Hamil-

tonian \hat{H} in the basis $|j, k\rangle$ are given by

$$\langle j, k | \hat{H} | j, k \rangle = \frac{\hbar^2}{4}(a+b)(j(j+1) - k^2) + \frac{\hbar^2}{2}ck^2, \quad (2)$$

$$\begin{aligned} \langle j, k | \hat{H} | j, k+2 \rangle &= \langle j, k+2 | H | j, k \rangle = \\ &= \frac{\hbar^2}{8}(a-b)\sqrt{(j-k)(j-k-1)(j+k+1)(j+k+2)}. \end{aligned} \quad (3)$$

For a fixed value of j , the Hamiltonian matrix can be decomposed in four submatrices, corresponding to different classes of symmetry.⁹ The numerical diagonalization of the matrix gives the "exact" energy levels of triaxial rigid rotator.⁶

3 Semiclassical description

It is important to observe that, also if the "exact" energy spectrum of the triaxial rigid rotator cannot be analytically determined, the classical Hamiltonian of the triaxial top is integrable.^{7,8} We use the classical integrability of our triaxial top to calculate the semiclassical energy spectrum via torus quantization. The first step is to find out the action variables of the Hamiltonian. By using the Deprit transformation⁸ (this is also known, at the quantum level, as Villain's representation of angular momentum¹⁰

$$J_1 = \sqrt{J^2 - J_3^2} \sin \theta, \quad J_2 = \sqrt{J^2 - J_3^2} \cos \theta, \quad (4)$$

where $J^2 = J_1^2 + J_2^2 + J_3^2$, the classical Hamiltonian can be written as

$$H = \frac{1}{2}aJ^2 + \frac{1}{2}[(c-a) - (b-a)\cos^2\theta] J_3^2 + \frac{1}{2}(b-a)J^2\cos^2\theta, \quad (5)$$

where the dynamical variable J_3 is the action variable of the angle θ .⁸ By performing another canonical transformation the angular dependence of the Hamiltonian $H = H(J, J_3, \theta)$ can be removed. Thus the Hamiltonian can be written as a function of two action variables: the total angular momentum J and a new action variable I given by

$$I = \frac{J}{\pi} \int_{\theta_1}^{\theta_2} \sqrt{\frac{2H}{J^2} - a - (b-a)\cos^2\theta \over (c-a) - (b-a)\cos^2\theta} d\theta. \quad (6)$$

The Hamiltonian H is now an implicit function of two action variables: $H = H(J, I)$. It means that the system is integrable and the classical trajectories of the 6-dimensional phase-space are restricted to a 2-dimensional torus.⁷ For a fixed value of J the Hamiltonian (5) describes a sort of nonlinear pendulum where the extrema of integration are

$$\theta_1 = \arccos \left[\sqrt{\frac{2H - aJ^2}{2(b-a)}} \right], \quad \theta_2 = \arccos \left[-\sqrt{\frac{2H - aJ^2}{2(b-a)}} \right], \quad (7)$$

for $0 \leq H < (b/2)J^2$ and it corresponds to librational motion, while they are

$$\theta_1 = 0, \quad \theta_2 = \pi, \quad (8)$$

for $(b/2)J^2 < H \leq (c/2)J^2$ and it corresponds to rotational motion. Note that $H = (b/2)J^2$ is the energy of the separatrix between librational and rotational motions. The semiclassical (torus) quantization¹¹ of the energy is performed by setting

$$J = \left(j + \frac{1}{2} \right) \hbar, \quad I = k\hbar, \quad (9)$$

where j and k are integer quantum numbers such that $k = -j, -j+1, \dots, j-1, j$ and $j \geq 0$. Note that only recently the corrections to this torus quantization, namely the higher order terms of the WKB series of the angular momentum, have been investigated.¹² For a fixed value of j there is a set of $2j+1$ energy levels but the semiclassical energy spectrum $E_{j,k}^{sc}$, given by the implicit equation

$$k\hbar = \frac{1}{\pi} \left(j + \frac{1}{2} \right) \hbar \int_{\theta_1}^{\theta_2} \sqrt{\frac{2\epsilon_{j,k}^{sc} - a - (b-a)\cos^2\theta}{(c-a) - (b-a)\cos^2\theta}} d\theta, \quad (10)$$

where $\epsilon_{j,k}^{sc} := E_{j,k}^{sc}/[(j+1/2)^2\hbar^2]$, has j couples of degenerate levels because $E_{j,k}^{sc} = E_{j,-k}^{sc}$. The lowest energy level of the set is $E_{j,0}^{sc} = a\hbar^2(j+1/2)^2/2$ while the higher is $E_{j,j}^{sc} = c\hbar^2(j+1/2)^2/2$.

4 Numerical results: spectral fluctuations

In Figure 1 we compare the "exact" energy spectrum, obtained with the numerical diagonalization⁶ of the matrix Hamiltonian given by Eq. (2) and Eq.

(3), with the semiclassical one, calculated using Eq. (10). As expected, the semiclassical quantization cannot take into account the broken degeneracy of pairs of “exact” energy levels. Moreover we find that the semiclassical energy levels are more accurate in the higher part of the spectrum (rotational levels).

Berry and Tabor^{1,2} have shown that for classically integrable systems the spectral statistics $P(s)$ and $\Delta_3(L)$ are expected to follow Poisson predictions: $P(s) = \exp(-s)$ and $\Delta_3(L) = \frac{L}{15}$. These predictions are based on the analysis of the semiclassical energy spectrum of a generic integrable Hamiltonian with more than one action variable. Thus, to test the Berry-Tabor theory, is much more appropriate to investigate spectral statistics of the semiclassical energy levels than spectral statistics of “exact” energy levels, as done in Ref. 6.

In Figure 2 we plot $P(s)$ and $\Delta_3(L)$ obtained from the semiclassical energy spectrum. The level spectrum is mapped into unfolded levels with quasi-uniform level density by using a standard procedure described in Ref. 13. $P(s)$ is the distribution of nearest-neighbor spacings $s_i = (\tilde{E}_{i+1} - \tilde{E}_i)$ of the unfolded levels \tilde{E}_i . It is obtained by accumulating the number of spacings that lie within the bin $(s, s + \Delta s)$ and then normalizing $P(s)$ to unit. The statistic $\Delta_3(L)$ is defined, for a fixed interval $(-L/2, L/2)$, as the least-square deviation of the staircase function $N(E)$ from the best straight line fitting it, where $N(E)$ is the number of levels between E and zero for positive energy, between $-E$ and zero for negative energy. Figure 3 shows that the spectral distribution $P(s)$ has a peak near $s=1$ and nothing elsewhere. The spectral rigidity $\Delta_3(L)$ follows the Poisson prediction $\Delta_3(L) = L/15$ for small L but for larger values of L it gets a constant mean value with fluctuations around this mean value.

The results of Figure 2 and Figure 3 can be explained in the following way. As shown in the previous section, fixing the angular momentum J the triaxial rigid rotator is one-dimensional: in the case of systems with only one action variable the energy spectrum is locally harmonic and, after unfolding, the spectral fluctuations have the pathological behavior of the one-dimensional harmonic oscillator, thus the spacings are all close to one. Moreover, it is important to observe that both “exact” and semiclassical levels have a linear grow apart near the separatrix where they cluster. This effect is shown in Figure 3 and Figure 4 where we plot the true nearest neighbor spacings (without unfolding) of semiclassical and “exact” energy levels as a function of the energy for a fixed value of the angular momentum. The spacings of the

semiclassical energy levels decrease quasi-linearly with the energy up to the separatrix and then they increase quasi-linearly. The same behavior is found for the spacings of the “exact” energy levels. In particular, in Figure 4 we plot the spacings of the exact energy levels corresponding to the four classes of symmetry of the system: the total Hamiltonian matrix is decomposed in the direct product of 4 submatrices by considering the parity of the quantum number k : even (E) or odd (O), and the symmetry of the state: symmetric (S) or anti-symmetric (A). So the submatrices are labelled as follow: (E,S), (E,A), (O,S), (O,A). These are the classes of symmetry of the system.^{6,9} Note that the spacings of each class of symmetry have the same trend but there are some fluctuations, in particular around the extrema of the energy spectrum. We have verified that these results do not depend on the choice of the inertia parameters of the asymmetric rigid rotator.

5 Algebraic Harmonic Approximation close to minima and maxima: single levels

The investigation of the triaxial-top classical Hamiltonian with $a < b < c$ reveals that the minimum-energy configuration is doubly realized by $(J_1, J_2, J_3) = (\pm J, 0, 0)$, where J is the radius of the sphere $J_1^2 + J_2^2 + J_3^2 = J^2$ and represents a constant of motion. On the other hand, the configurations $(J_1, J_2, J_3) = (0, 0, \pm J)$ and $(J_1, J_2, J_3) = (0, \pm J, 0)$ are recognized to be maxima and saddle points, respectively. By using the Casimir operator \hat{J}^2 , we notice that the quantum Hamiltonian \hat{H} can be rewritten in the two forms

$$\hat{H} = \frac{1}{2} \left[a\hat{J}^2 + (b-a)\hat{J}_2^2 + (c-a)\hat{J}_3^2 \right], \quad (11)$$

$$\hat{H} = \frac{1}{2} \left[c\hat{J}^2 - (c-a)\hat{J}_1^2 - (c-b)\hat{J}_2^2 \right], \quad (12)$$

close to the minima and the maxima, respectively. The observation that, classically, the energy minimum is reached for $J_2 = J_3 = 0$, and $J_1 = \pm J$, leads to approximate J_1 as $J_1 \simeq \pm J[1 - (J_2^2 + J_3^2)/2J^2]$. This implies, at the quantum level, the inequalities $\langle \hat{J}_s \rangle \ll J$ [where the radius J is given quantally by $J^2 = j(j+1)\hbar$] concerning the expectation values of \hat{J}_s ($s = 2, 3$) and makes natural to adopt the perturbative scheme (see Ref. 14) in which

the operator \hat{J}_2 and \hat{J}_3 can be treated as canonically conjugate variables. Such a feature follows from

$$[\hat{J}_2, \hat{J}_3] \simeq iJ, \quad (13)$$

whereas

$$[\hat{J}_3, \hat{J}_1] = iJ(\hat{J}_2/J) \simeq 0, \quad [\hat{J}_1, \hat{J}_2] = iJ(\hat{J}_3/J) \simeq 0, \quad (14)$$

are considered vanishing when compared with (13) since $\langle \hat{J}_s \rangle / J \ll 1$. Then, after labeling by the integer k the eigenstates of the harmonic oscillator term $(c-a)[\hat{J}_3^2 + W^2 \hat{J}_2^2]$ contained in \hat{H} , where $W^2 = (b-a)/(c-a)$, its eigenvalues are found to be $JW(2k+1)$ so that the spectrum of \hat{H} reads

$$E_{j,k}^{har} = \frac{1}{2} \left[aj(j+1)\hbar^2 + \sqrt{j(j+1)\hbar} \sqrt{(b-a)(c-a)} (2k+1)\hbar \right]. \quad (15)$$

The approximation just implemented is not consistent with the spectrum expected for $c \rightarrow a$. In fact, in such a case the Hamiltonian becomes $\hat{H} = [cJ^2 + (b-a)\hat{J}_1^2]/2$ thus entailing however a quadratic spectrum $E = [cJ^2 + (b-a)k^2\hbar^2]/2$. Similarly, the approximation for the maxima is obtained by noticing that $J_3 \simeq \pm J[1 - (\hat{J}_1^2 + \hat{J}_2^2)/2J^2]$, and

$$[\hat{J}_1, \hat{J}_2] \simeq iJ, \quad (16)$$

$$[\hat{J}_3, \hat{J}_1] = iJ(\hat{J}_2/J) \simeq 0, \quad [\hat{J}_2, \hat{J}_3] = iJ(\hat{J}_1/J) \simeq 0. \quad (17)$$

In this case, the harmonic oscillator term $(c-b)[\hat{J}_2^2 + \Omega^2 \hat{J}_1^2]$, with $\Omega^2 = (c-a)/(c-b)$, contained in \hat{H} leads to the spectrum

$$E_{j,k}^{har} = \frac{1}{2} \left[cj(j+1)\hbar^2 - \sqrt{j(j+1)\hbar} \sqrt{(c-a)(c-b)} (2k+1)\hbar \right], \quad (18)$$

which differs from Eq. (15) owing to the interlevel separation. In Figure 5 we compare "exact" energy levels with those obtained using the harmonic approximation. The results show that indeed the harmonic approximation is quite accurate, also better than the semiclassical one, close to the minimum and the maximum of the energy.

Conclusions

In this paper we have investigated the energy spectrum of the triaxial rigid rotator, a very important model for both atomic and nuclear physics. We have found that its semiclassical energy spectrum is spanned by two quantum numbers: the quantum number j of the total angular momentum J and the quantum number k of the other action variable I of the system. For a fixed value of j the semiclassical energy spectrum depends on the quantum number k and can be divided into librational and rotational energy levels. Moreover, the spacings of both “exact” and semiclassical energy spectra show a quasi-linear behavior as a function of energy: nearest neighbour spacings have a quasi-linear decrease up to the energy of the separatrix and then a quasi-linear increase. We have also shown that the semiclassical energy spectrum is in good agreement with the “exact” one, but cannot take into account the broken degeneracies of pairs of “exact” energy levels. From our analysis it follows that the spectral fluctuations of the asymmetric top have the pathological behavior of the one-dimensional harmonic oscillator. This effect has been verified by calculating the spectral statistics $P(s)$ and $\Delta_3(L)$. Finally, we have deduced analytical formulas, based on an algebraic approximation of the quantum Hamiltonian, which describe remarkably well the energy levels of the triaxial rotor close to extrema of the energy.

V.R.M. is greatly indebted to M.V. Berry, S. Graffi and A. Turchetti for many suggestions at different stages of the paper. L.S. thanks T. Prosen for enlightening discussions.

References

1. M.V. Berry and M. Tabor, Proc. Roy. Soc. Lond. A **356**, 375 (1977); M.V. Berry, Annals of Phys. **131**, 163 (1981); M.V. Berry, Proc. Roy. Soc. Lond. A **400** 229 (1985).
2. M. Tabor, *Chaos and Integrability in Nonlinear Dynamics* (Wiley, New York, 1989).
3. V.R. Manfredi and L. Salasnich, Int. J. Mod. Phys. B **13**, 2343 (1999).
4. A. Pandey, O. Bohigas and M.J. Giannoni, J. Phys. A: Math. Gen. **22** 4083 (1989).

5. A. Pandey and R. Ramaswamy, Phys. Rev. A **43**, 4237 (1991).
6. V.R. Manfredi and L. Salasnich, Phys. Rev. E **64**, 066201 (2001).
7. V.I. Arnold, *Mathematical Methods in Classical Mechanics* (Springer, New York, 1984).
8. A.R.P. Rau, Rev. Mod. Phys. **64** 623 (1992); A. Turchetti, *Dinamica Classica dei Sistemi Fisici* (Zanichelli, Bologna, 1998)
9. L. Landau and E. Lifshitz, *Course in Theoretical Physics*, vol. 3: Quantum Mechanics (Pergamon, London, 1977).
10. J. Villain, J. de Phys. **35**, 27 (1974).
11. V.P. Maslov and M.V. Fedoriuk, *Semiclassical Approximation in Quantum Mechanics* (Reidel Publishing Company, New York, 1981)
12. M. Robnik and L. Salasnich, J. Phys. A (Math. Gen.) **30**, 1719 (1997); L. Salasnich and F. Sattin, J. Phys. A (Math. Gen.) **30**, 7597 (1997); M. Robnik and L. Salasnich, Nonlinear Phenomena in Complex Systems **3**, 99 (2000).
13. V.R. Manfredi, Lett. Nuovo Cimento **40**, 135 (1984).
14. R. Franzosi, V. Penna and R. Zecchina, Int. J. Mod. Phys. B **14**, 943 (2000).

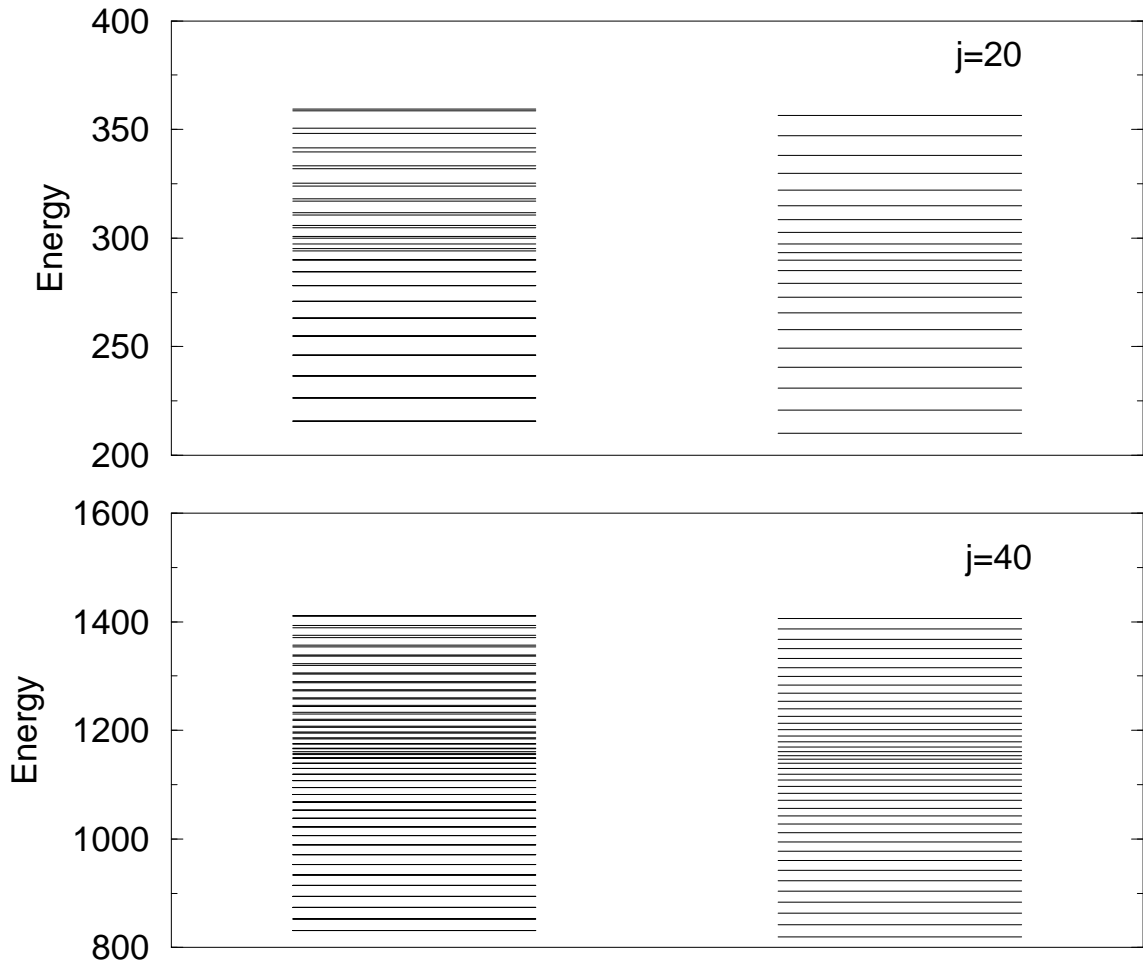


Fig. 1: “Exact” (left) vs semiclassical (right) energy spectrum of the triaxial rigid rotator with a fixed value of the angular momentum j . Parameters: $a = 1$, $b = \sqrt{2}$, $c = \sqrt{3}$ and $\hbar = 1$. Energy in arbitrary units.

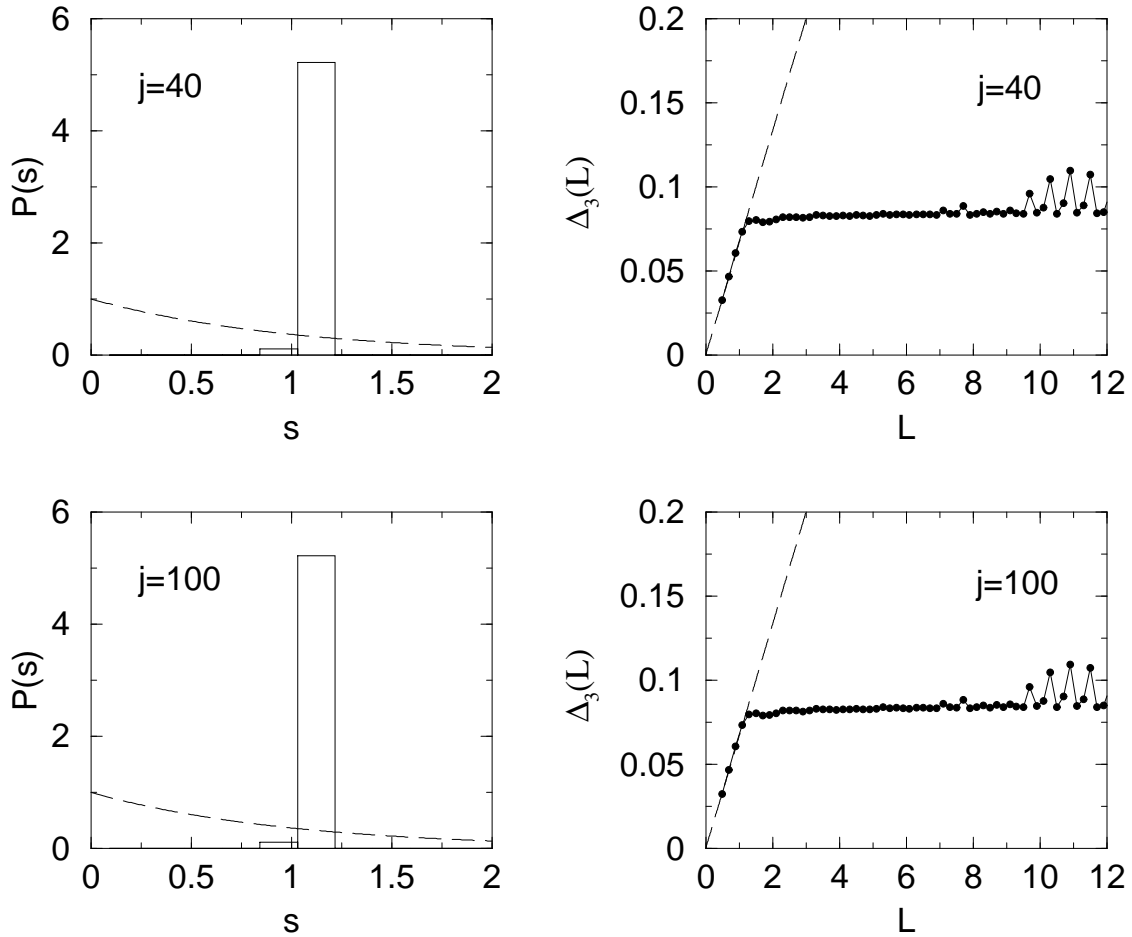


Fig. 2: Nearest neighbor spacing distribution $P(s)$ and spectral rigidity $\Delta_3(L)$ of the semiclassical energy spectrum of the triaxial rigid rotator with a fixed value of the angular momentum j . The dashed lines are the Poisson predictions: $P(s) = \exp(-s)$ and $\Delta_3(L) = L/15$. Parameters as in Figure 1

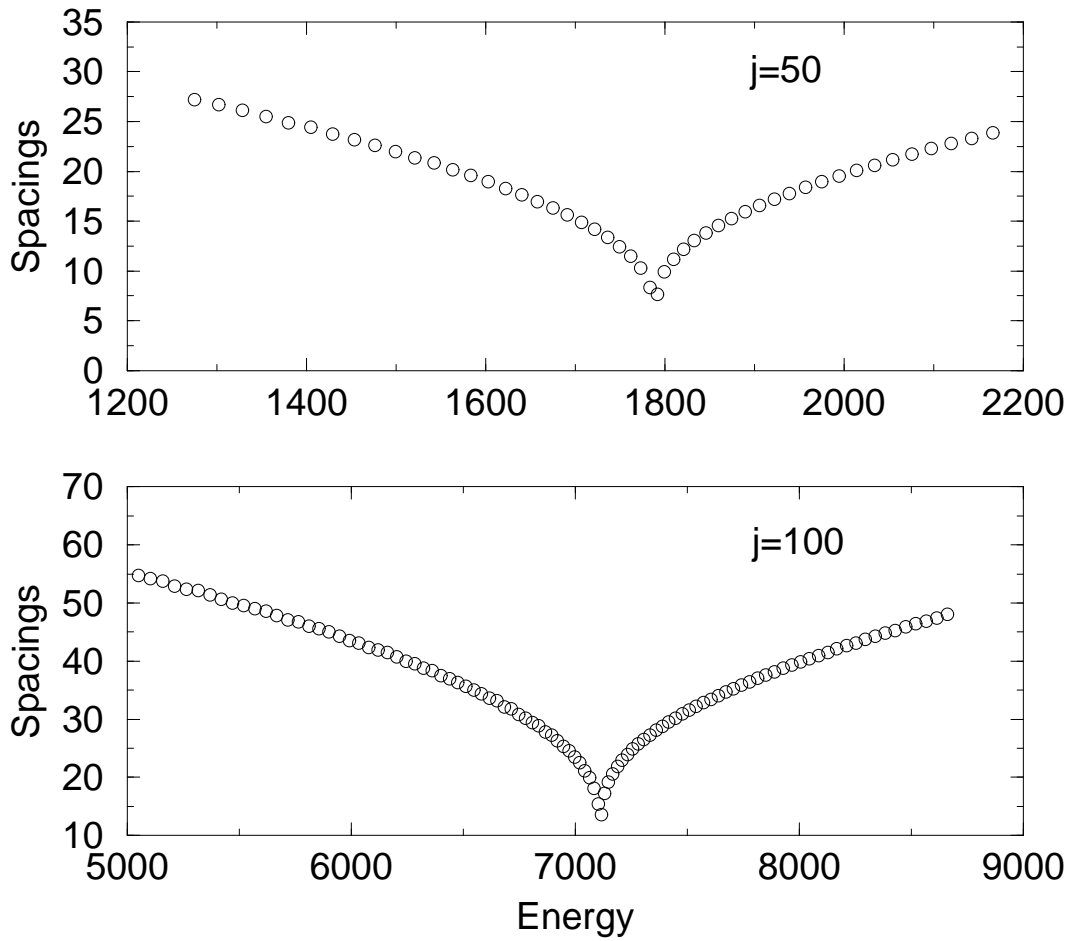


Fig. 3: True spacings (without unfolding) as a function of energy. Semiclassical energy levels of the triaxial rigid rotator for two values of the angular momentum j . Parameters and units as in Figure 1.

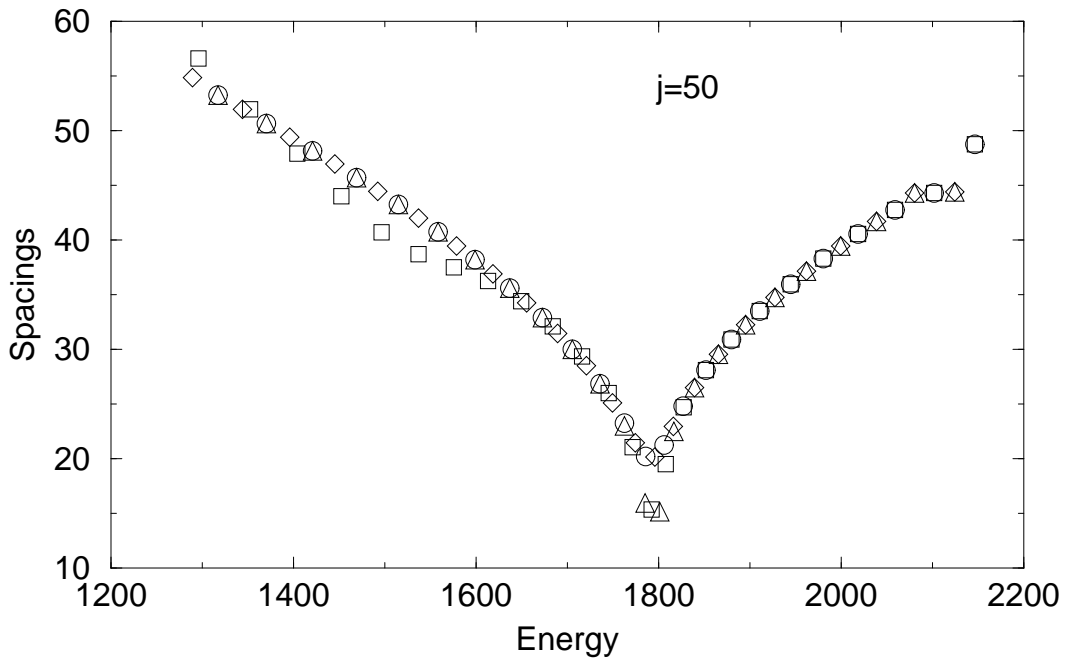


Fig. 4: True spacings (without unfolding) as a function of energy. “Exact” energy levels of the triaxial rigid rotator for a fixed value of the angular momentum j . Four classes of symmetry: square for class (E,S), circle for class (E,A), diamond for class (O,S), triangle for class (O,S). Parameters and units as in Figure 1.

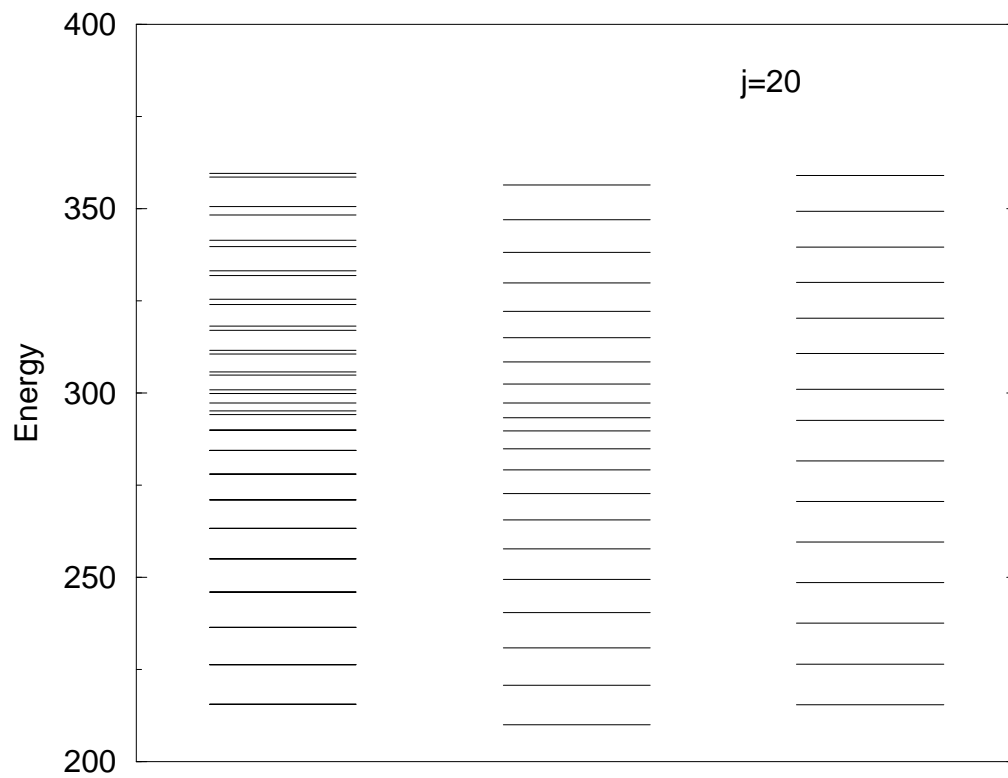


Fig. 5: “Exact” (left), semiclassical (middle) and harmonic-approximation (right) energy spectrum of the triaxial rigid rotator with a fixed value of the angular momentum j . Parameters and units as in Figure 1.